Cell

The GATA2 Transcriptional Network Is Requisite for RAS Oncogene-Driven Non-Small Cell Lung Cancer

Madhu S. Kumar,[1] David C. Hancock,[1,8] Miriam Molina-Arcas,[1,8] Michael Steckel,[1] Phillip East,[2] Markus Diefenbacher,[3] Elena Armenteros-Monterroso,[1] François Lassailly,[4] Nik Matthews,[5] Emma Nye,[6] Gordon Stamp,[6] Axel Behrens,[3] and Julian Downward[1,7,*]

[1]Signal Transduction Laboratory
[2]Bioinformatics and Biostatistics Group
[3]Mammalian Genetics Laboratory
[4]In-Vivo Imaging Facility
[5]Advanced Sequencing Facility
[6]Experimental Histopathology Laboratory
Cancer Research UK London Research Institute, 44 Lincoln's Inn Fields, London WC2A 3LY, UK
[7]The Institute of Cancer Research, 237 Fulham Road, London SW3 6JB, UK
[8]These authors contributed equally to this work
*Correspondence: julian.downward@cancer.org.uk
DOI 10.1016/j.cell.2012.02.059

SUMMARY

Non-small cell lung cancer (NSCLC) is the most frequent cause of cancer deaths worldwide; nearly half contain mutations in the receptor tyrosine kinase/RAS pathway. Here we show that RAS-pathway mutant NSCLC cells depend on the transcription factor GATA2. Loss of GATA2 reduced the viability of NSCLC cells with RAS-pathway mutations, whereas wild-type cells were unaffected. Integrated gene expression and genome occupancy analyses revealed GATA2 regulation of the proteasome, and IL-1-signaling, and Rho-signaling pathways. These pathways were functionally significant, as reactivation rescued viability after GATA2 depletion. In a Kras-driven NSCLC mouse model, Gata2 loss dramatically reduced tumor development. Furthermore, Gata2 deletion in established *Kras* mutant tumors induced striking regression. Although GATA2 itself is likely undruggable, combined suppression of GATA2-regulated pathways with clinically approved inhibitors caused marked tumor clearance. Discovery of the nononcogene addiction of *KRAS* mutant lung cancers to GATA2 presents a network of druggable pathways for therapeutic exploitation.

INTRODUCTION

Lung cancer is the most prevalent cancer type worldwide by both diagnosis and mortality, with non-small cell lung cancer (NSCLC) featuring as the most common histological subtype (Ferlay et al., 2010). Among NSCLC patients, the most frequently mutated oncogenes are the RAS family of GTPases and various receptor tyrosine kinases (RTKs), constituting nearly half of all NSCLCs. Though mutations in the RAS family in human cancers have been known for 30 years, therapeutic targeting of RAS has so far proven intractable. Moreover, although tyrosine kinase inhibitors exhibit striking efficacy in NSCLC patients with mutant RTKs, patients inevitably develop therapeutic resistance. Thus, novel therapies are needed to target RAS-pathway mutant NSCLCs.

One potentially promising approach has been to target pathways acting downstream of RAS: combined inhibition of ERK and PI 3-kinase pathways with small-molecule inhibitors can impair the growth of *Kras* mutant mouse lung tumors (Engelman et al., 2008). Moving beyond direct RAS effectors, several groups have screened for factors and pathways necessary for *KRAS* mutant cancer cell survival. An initial candidate was the TANK-binding kinase 1 (TBK1), found in a short hairpin RNA (shRNA) screen of the kinome (Barbie et al., 2009). In *RAS* mutant cells, RalB activates TBK1, which maintains survival through activation of the NF-κB pathway, a signaling cascade found to be necessary in a mouse model of mutant Kras-driven NSCLC (Chien et al., 2006; Meylan et al., 2009).

Beyond antiapoptotic factors, several groups have found targets that promote *KRAS* mutant cancers via maintenance of cellular proliferation. One of the initial mutant *KRAS* synthetic lethal shRNA screens found mitotic regulators to be specifically necessary for mutant cell fitness (Luo et al., 2009). Conversely, Barbacid and colleagues found that both human cancer cells and a mutant *Kras* mouse model depend on the G_1/S regulator Cdk4 (Puyol et al., 2010). Moreover, functional analysis of an oncogenic KRAS expression signature revealed the Wilms' tumor gene WT1 to be required in mutant *KRAS* cells via

regulation of cellular senescence (Vicent et al., 2010). In sum, these studies suggest a broad role for cell-cycle control in oncogenic KRAS-mediated tumorigenesis.

Although these investigations suggest various candidates for RAS-pathway mutant dependency in NSCLC, several important issues require deeper investigation. First, it is unclear whether these factors are required only in *KRAS* mutant cancer cells or more broadly in cancers that activate the RAS-signaling pathways, like activated RTKs or inactivated RAS GTPase-activating proteins (GAPs). Second, these candidates have generally focused on single processes upon which *KRAS* mutant cancer cells might depend. Single targeting of candidates and pathways will likely only transiently suppress tumorigenesis due to the development of resistance. Consequently, combination treatments that inhibit multiple dependencies might prove a more efficacious therapeutic route. Third, although these targets were shown to be required in mutant cancer cells, the effect of whole-body loss of these targets in the context of the tumor has in many cases not been described. Because any potential therapeutic agent will likely operate throughout the patient, it is important to determine what toxicities might be presented by target inhibition in the organismal milieu. In addition, the previous in vivo studies described have generally focused on tumor development—the effect on forming the tumor in the absence of the target—and not on the more clinically relevant issue of tumor maintenance—the effect of disabling the target in a preformed tumor. Finally, most of the previously described screens, though generating candidate factors for drug development, have not provided novel therapeutic strategies derived from clinically licensed inhibitors. Considering the significant time required for drug development and testing, it would be intriguing to envisage therapeutic regimens with compounds already in clinical use.

Here we describe the transcription factor GATA2 as required for the survival of RAS-pathway mutant NSCLC. Both in vitro and in vivo, loss of GATA2 reduces mutant NSCLC cell line viability. Combined gene expression and chromatin occupancy analysis reveals a broad network of pathways controlled by GATA2 in RAS-pathway mutant NSCLC cells. These pathways are salient to GATA2-mediated survival, as their reactivation restores viability in response to GATA2 depletion. Furthermore, Gata2 is required for *Kras* mutant tumorigenesis in an autochthonous mouse model, and whole-organism loss of Gata2 induces regression of established *Kras* mutant lung tumors without drastic toxicities. Finally, combined inhibition of GATA2-regulated pathways with clinically available inhibitors recapitulates the effect of GATA2 loss, causing a robust suppression of established *Kras* mutant NSCLC and providing an immediately applicable therapeutic strategy for RAS-pathway mutant NSCLC.

RESULTS

KRAS Mutant NSCLC Cells Specifically Require GATA2 for Survival

To discover novel genes necessary in *KRAS* mutant cancer cells, we performed an RNA interference (RNAi) screen targeting some 7,000 human genes in a panel of *KRAS* mutant and wild-type (WT) cancer cells. Among other factors (including KRAS itself), we found that loss of the transcription factor GATA2 led to a decrease in *KRAS* mutant cell viability and an increase in apoptosis (M.S., M.M.-A., D.C.H., and J.D., unpublished data). To extend these findings, we analyzed 26 NSCLC cell lines, of which 14 were *KRAS* mutant and 12 were WT. Short-term GATA2 knockdown led to specific decreased cell viability and increased apoptosis in *KRAS* mutant NSCLC cells, comparable to the effect seen with loss of KRAS itself (Figure 1A and Figure S1A available online). Comparison of expression across the panel revealed no significant differences in GATA2 expression between mutant and WT cells (data not shown). Interestingly, the relative effect of GATA2 loss on viability correlated with the extent of GATA2 knockdown in mutant but not WT cells (Figure S1B). Moreover, there was a modest relationship between the effect of GATA2 knockdown and that of KRAS knockdown in mutant but not WT cells ($p < 0.05$ for *KRAS* mutant cells by Pearson's correlation). Also, comparison of the effect of GATA2 depletion in the panel with other frequent mutations in NSCLC (such as *TP53*, *STK11*, and *CDKN2A*) revealed no significant delineations, emphasizing the specific role for mutant *KRAS* in GATA2 dependency (Figure S1C). Taken together, these findings suggest that *KRAS* mutant NSCLC cells depend upon GATA2 for survival.

GATA2 Is Necessary for the Viability of RAS-Pathway Mutant NSCLC Cells

Although the above findings demonstrate that GATA2 was required in NSCLC cells with mutations in known RAS-pathway components, it was unclear whether this dependency occurred in NSCLCs containing other mutant oncogenes, such as RTKs like epidermal growth factor receptor (*EGFR*). To address this, we used small-interfering RNAs (siRNAs) against both KRAS and GATA2 in the NSCLC cell lines A549 (*KRAS* mutant), PC9 (*EGFR* mutant), and H322M (WT). As expected, A549 cells exhibited reduced viability with loss of either KRAS or GATA2, whereas H322M cells were unaffected (Figure 1B). Surprisingly, PC9 cells were also dependent on GATA2 for viability. Examination of additional *EGFR* mutant (H3255) and *KRAS* mutant (H441) NSCLC cells revealed similar effects for GATA2 (Figure S1D). Importantly, both KRAS and GATA2 were knocked down effectively with the siRNAs (Figure S1E). In sum, these findings suggest that GATA2 is broadly required in the survival of RAS-pathway mutant NSCLC.

To further validate GATA2, we designed shRNAs against GATA2. To this end, one shRNA (shGATA2.1) achieved substantial knockdown of GATA2 in A549 and PC9 cells relative to a control (shGAPDH) and a nonfunctional GATA2 shRNA (shGATA2.2) (Figure 1C). Notably, shGATA2.1-expressing A549 and PC9 cells had greatly reduced viability relative to the other shRNAs but did not affect WT H322M cells (Figure 1D). Hereafter, shGATA2.1 is referred to as "shG" and shGAPDH as "shC."

Examination of additional *KRAS* and *EGFR* mutant cells showed a striking dependency on GATA2 for mutant cell viability (Figure S1F). Moreover, this dependency was broadly observed in oncogene-driven NSCLC cells, as cell lines with mutations in *NRAS*, *NF1*, and *EML4-ALK* all exhibited reduced viability in response to GATA2 knockdown. In contrast, WT NSCLC cells

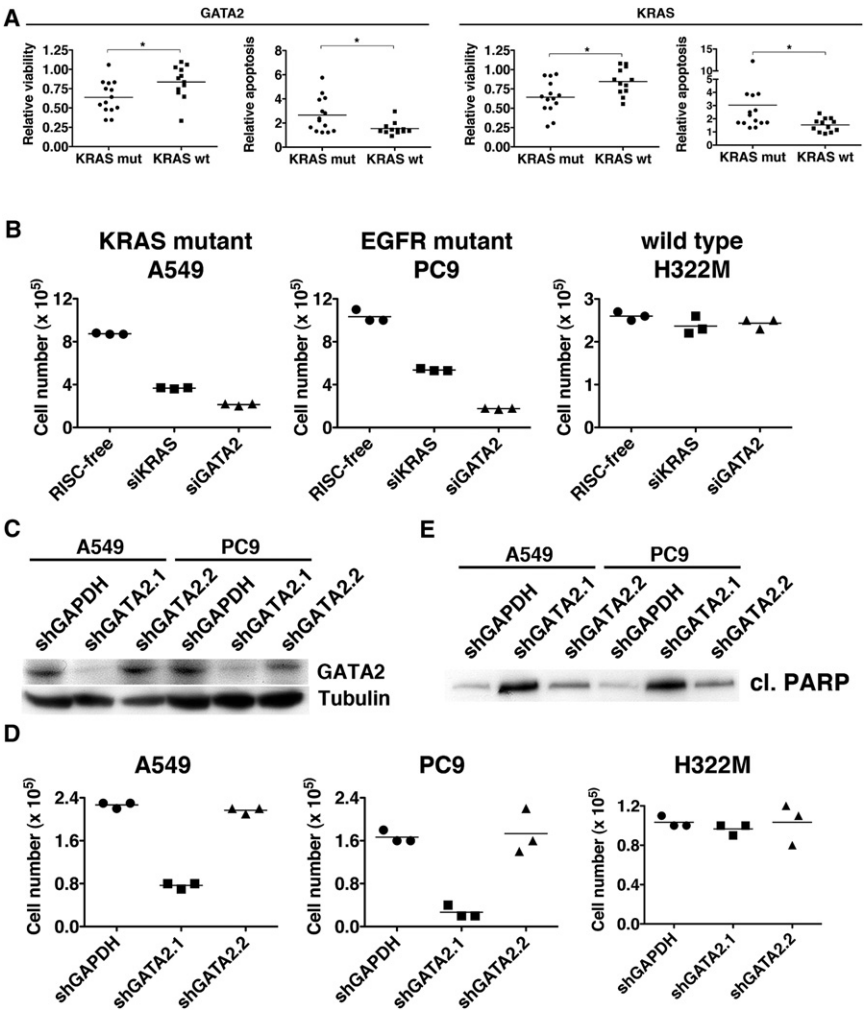

Figure 1. GATA2 Is Required in RAS-Pathway Mutant NSCLC

(A) Fourteen *KRAS* mutant and twelve *KRAS* WT NSCLC lines were transfected with control siRNA, siRNA targeting GATA2, or siRNA targeting KRAS. Cell titer blue and APO-one assays were used to measure viability and apoptosis, respectively. $^{*}p < 0.05$.

(B) *KRAS* mutant (A549), *EGFR* mutant (PC9), and WT (H322M) NSCLC cells were transfected with control siRNA (RISC-free), KRAS siRNA, or GATA2 siRNA. Cell numbers were counted 72 hr later.

(C) shRNAs targeting GAPDH (shGAPDH) and GATA2 (shGATA2.1 and shGATA2.2) were infected into A549 and PC9 cells, followed by western blotting for GATA2 and tubulin.

(D) ShRNA-infected A549, PC9, and H322M cells were plated, and cell numbers were counted as above.

(E) Western blotting was performed on shRNA-infected A549 and PC9 cells for cleaved PARP. See also Figure S1.

were unaffected by GATA2 depletion (Figure S1G). Importantly, RAS-pathway mutant and WT lung cancer cells express comparable amounts of GATA2 and exhibit similar levels of knockdown with the shRNA (Figure S1H). To resolve off-target effects of the shRNA, we rescued GATA2 expression with a GATA2 cDNA in which the shRNA-binding site had been mutated to prevent knockdown (Figure S1I). Notably, the shRNA-mutated cDNA achieves a near-complete rescue of viability, demonstrating the specificity of the effect on GATA2 loss (Figure S1J). Moreover, to determine whether this dependency was conserved from human to mouse lung cancer cells, we generated shRNAs targeting murine Gata2. These shRNAs achieved substantial knockdown of GATA2 and caused a striking decrease in the growth of a murine *Kras* mutant NSCLC cell line (Figures S1K and S1L).

These results indicate that GATA2 loss reduces RAS-pathway mutant cell viability but do not indicate whether this effect is due to increased apoptosis or impaired proliferation. Thus, we examined both apoptotic markers and the cell-cycle distribution in GATA2 knockdown cells. With GATA2 depletion in mutant lung cancer cells, we observed elevated PARP cleavage, a marker of apoptotic cell death (Figure 1E). Conversely, we observed no significant change in the cell-cycle profiles of mutant cancer cells with GATA2 knockdown (Figure S1M). Taken together, these results show that GATA2 is necessary for the survival of RAS-pathway mutant NSCLC.

GATA2 Is Necessary for Oncogene-Driven Lung Cancer Growth In Vivo

Although the above studies revealed that GATA2 is required for RAS-pathway mutant NSCLC viability in vitro, it was unclear whether this was maintained in vivo. Thus, we examined the ability of GATA2-depleted lung cancer cells to alter tumor xenograft growth. As seen in Figure 2A, injection of control shRNA-expressing RAS-pathway mutant NSCLC cells led to robust tumor growth. In contrast, GATA2 knockdown cells completely abrogated tumor formation, with no detectable lesions forming over 9 months. The effect of GATA2 on RAS-pathway mutant tumors was specific, as loss of GATA2 had no impact on tumor growth in WT NSCLC cells (Figure 2B). Collectively, these results indicate that GATA2 is crucial for tumorigenesis in RAS-pathway mutant lung cancer.

GATA2 Regulates the Proteasome via Control of Nrf1

To elucidate the mechanisms by which GATA2 maintains RAS-pathway mutant NSCLC survival, we performed gene expression analysis on A549 and PC9 cells expressing either control or GATA2 shRNA. As GATA2 was likely to operate via broad regulatory nodes, gene set enrichment analysis (GSEA) was performed (a list of enriched gene sets is included in Figure S2A). One of the most striking candidate pathways negatively enriched in GATA2 knockdown cells was the proteasome pathway (Figure S2B). This was intriguing, as several screens

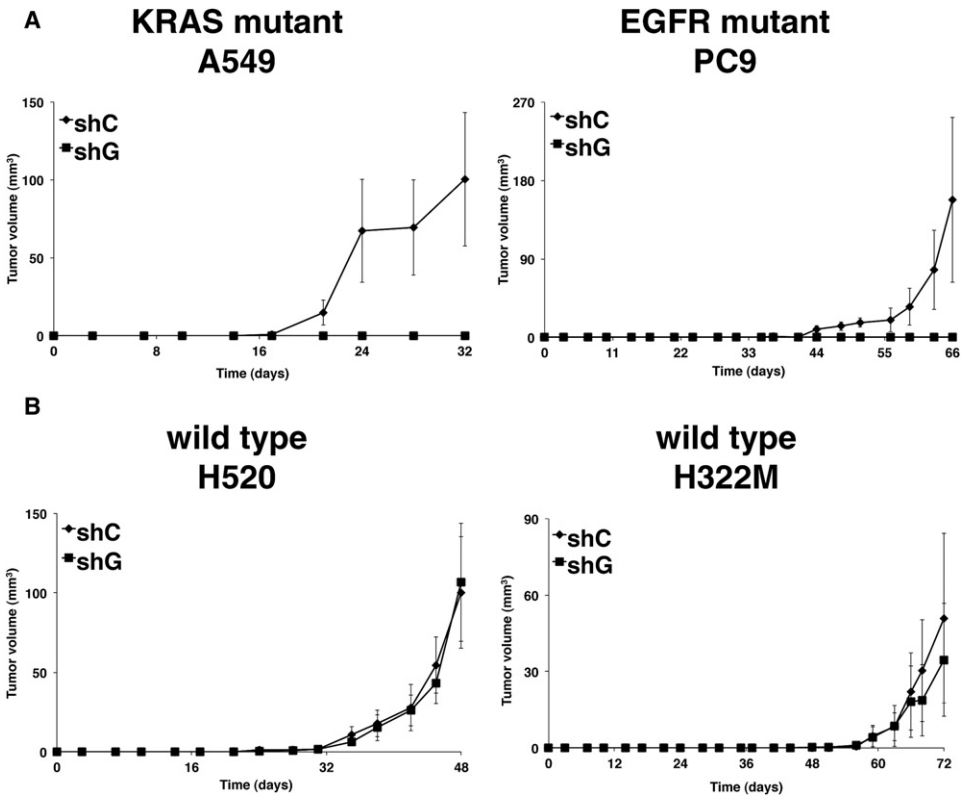

Figure 2. GATA2 Is Necessary for Oncogene-Driven Lung Tumorigenesis In Vivo

(A) A549 and PC9 cells infected with GAPDH (shC) and GATA2 (shG) shRNAs were injected subcutaneously into nude mice. Tumor volumes were measured with calipers. Values are mean ± SEM (n = 8).

(B) H520 and H322M cells infected with shRNAs were injected into nude mice as above. Values are mean ± SEM (n = 8).

for *KRAS* synthetic lethal factors revealed dependencies on components of the proteasome (Barbie et al., 2009; Luo et al., 2009). Because numerous proteasome components appeared downregulated with GATA2 loss, we suspected that transcriptional control of the proteasome was disrupted. Recent reports have described the transcription factor Nrf1 as a regulator of the proteasome (Radhakrishnan et al., 2010). Quantitative RT-PCR (qRT-PCR) revealed downregulation of Nrf1 and proteasome components with GATA2 knockdown independent of genotype (Figure 3A). Moreover, this transcriptional control was germane to proteasome function, as GATA2 loss impaired proteasome activity in mutant and WT NSCLC cells (Figure 3B).

To determine the role of the proteasome in GATA2-mediated survival, we expressed either Nrf1 or a dominant-negative form of the proteasome inhibitor USP14 ($USP14^{14}$) in RAS-pathway mutant cells (Lee et al., 2010). As seen in Figure 3C, expression of either dominant-negative USP14 or Nrf1 was functionally salient, as each re-established proteasome function after GATA2 depletion, with more robust rescue occurring in the $USP14^{SF}$ cells. Nrf1 was important for proteasome transcript levels, as it partially restored expression of several components (Figure S2C). After GATA2 loss, we observed a modest but discernible rescue of viability with both $USP14^{SF}$ and Nrf1 (Figure 3D); the variation in rescue is likely due to the incomplete restoration in proteasome expression by Nrf1, whereas $USP14^{SF}$ can posttranslationally elicit more complete rescue of proteasome function. Taken together, these findings suggest that proteasome function is sufficient for partial rescue of viability in response to GATA2 loss in RAS-pathway mutant NSCLC.

To examine further the dependency of RAS-pathway mutant lung cancer cells on the proteasome, we depleted proteasome components and inhibited the proteasome with bortezomib in our panel of *KRAS* mutant/WT NSCLC cells. We observed no significant differential viability with either proteasome component loss or bortezomib treatment (Figures S2D and S2E), although there is a slight tendency for mutant cells to be affected. Importantly, both approaches inhibited proteasome function comparably to GATA2 loss (Figure S2F). Taken together, these results indicate that proteasome inhibition is insufficient to differentially affect *KRAS* mutant NSCLC viability. Because of the failure of proteasome loss to differentially affect mutant cell viability, we wanted to ensure that the effects of GATA2 on the proteasome were on-target. To do so, we examined whether the shRNA-resistant GATA2 cDNA restored proteasome function. With the rescue system, we observed a complete reversal or proteasome inhibition, demonstrating that the effects of GATA2 on the proteasome are on-target (Figure S2G). We also

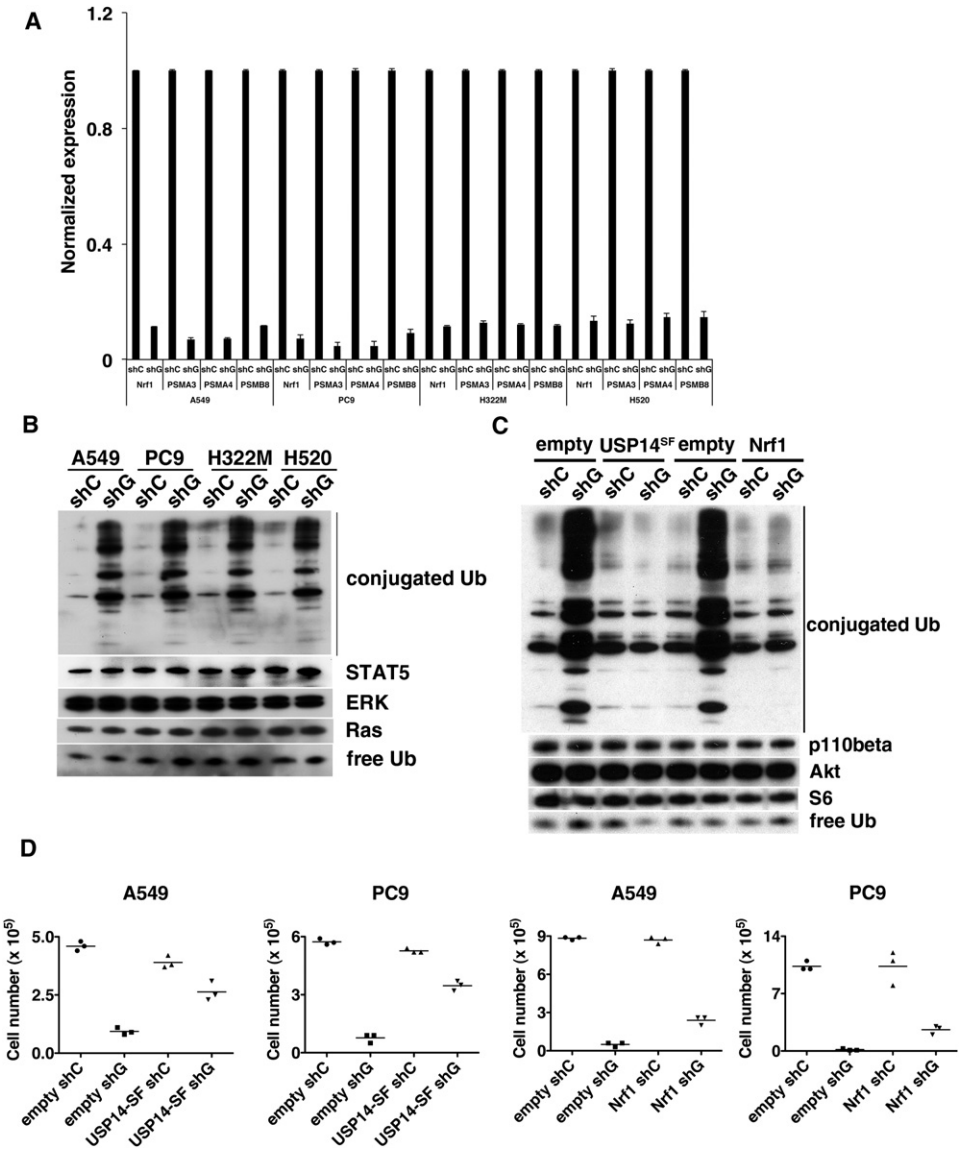

Figure 3. GATA2 Regulates Transcription of the Proteasome via Nrf1

(A) qRT-PCR was performed for a control transcript (PLK1), Nrf1, PSMA3, PSMA4, and PSMB8 in shRNA-infected A549, PC9, H322M, and H520 cells. Expression of target genes in shRNA cells was normalized to PLK1 levels. Target gene expression in shC cells was set to 1 to determine relative expression in shG cells. Values are mean ± SEM with propagated error (n = 3).

(B) Western blotting was performed on shRNA-infected A549, PC9, H322M, and H520 cells for ubiquitin (conjugated and free), STAT5, ERK, and RAS.

(C) Western blotting was performed on shRNA-infected A549 cells expressing empty vectors, dominant-negative USP14 ($USP14^{SF}$), or Nrf1 for ubiquitin (conjugated and free), p110beta, Akt, and S6.

(D) shRNA-infected A549 and PC9 cells expressing empty vectors, $USP14^{SF}$, or Nrf1 were plated and counted as in Figure 1D.

See also Figures S2 and S6.

assessed whether the effects on the proteasome were caused by elevated cell death by abrogating apoptosis with the caspase inhibitor z-VAD-fmk (z-VAD). Whereas z-VAD completely blocked the apoptosis induced by GATA2 loss, impaired proteasome function was maintained (Figures S2H and S2I). Collectively, these results suggest that the effects of GATA2 on the proteasome are not merely a consequence of apoptosis driven by GATA2 loss.

GATA2 Controls NF-κB Signaling through Regulation of the IL-1 Pathway

Beyond the proteasome, we noted a striking transcriptional repression of the IL-1- and NF-κB-signaling pathways with GATA2 depletion (Figure S3A). The differential expression was coupled to GATA2 genome occupancy, as chromatin immunoprecipitation coupled to next-generation sequencing (ChIP-seq) of GATA2 (to be discussed below) revealed enrichment of

IL-1 pathway genes like *TRAF6* (Figure S3B). Validation of GATA2 occupancy by ChIP-PCR revealed that GATA2 bound *TRAF6* only in RAS-pathway mutant cells, though it bound *PDK1* and *ZFPM2* across all lung cancer cells (Figure 4A). Moreover, only RAS-pathway mutant cells exhibited loss of TRAF6 expression after GATA2 knockdown (Figure 4B). Collectively, these findings indicate that GATA2 regulates expression of the IL-1 pathway in RAS-pathway mutant NSCLC.

We then assessed the consequence of this on the NF-κB pathway, an important downstream effector of IL-1 signaling (O'Neill, 2008). As seen in Figure 4C, we observed a remarkable suppression of an NF-κB pathway reporter in mutant lung cancer cells, with little change in WT cells. The reduction of NF-κB signaling was not downstream of GATA2-mediated apoptosis, as GATA2 knockdown similarly suppressed NF-κB activity when cell death was inhibited with z-VAD (Figure S3C). In sum, these results suggest that GATA2 is necessary for activation of the NF-κB cascade.

To determine a functional role for the IL-1 pathway in GATA2-mediated viability, we expressed TRAF6 in RAS-pathway mutant lung cancer cells, as TRAF6 overexpression exogenously activates IL-1 signaling (Cao et al., 1996). TRAF6 expression largely restored NF-κB signaling in response to GATA2 depletion (Figure 4D). Consequently, TRAF6 substantially rescued cell viability after GATA2 loss (Figure 4E). These effects were not due to TRAF6 regulation of GATA2 expression, as neither TRAF6 rescue nor TRAF6 depletion by siRNA altered GATA2 protein levels (Figures S3D and S3E). Overall, these findings demonstrate that GATA2 regulation of IL-1 signaling is functionally germane for RAS-pathway mutant cell survival.

Considering the substantial effect that the IL-1 pathway has on both NF-κB signaling and RAS-pathway mutant cell survival, we then evaluated the immediate role of NF-κB on GATA2-mediated viability. Expression of the NF-κB subunit RelA caused a striking rescue of NF-κB activity in response to GATA2 knockdown (Figure S3). Surprisingly, this only marginally affected viability after GATA2 depletion (Figure S3G). Moreover, we tested whether loss of either IL-1 or NF-κB signaling was sufficient to reduce mutant cell viability by depletion of TRAF6 or NEMO, an essential activator of canonical NF-κB signaling (Yamaoka et al., 1998). Though knockdown of either factor was able to suppress NF-κB signaling (Figure S3H), both caused only a modest reduction in viability (Figure 4F). Furthermore, inhibition of IL-1 signaling by the antagonist IL-1ra, although able to inhibit NF-κB activity (Figure S3I), had little effect on RAS-pathway mutant cell viability (Figure S3J). Collectively, these results demonstrate that whereas TRAF6 substantially rescues GATA2-mediated survival (to be discussed below), inhibition of either IL-1 or NF-κB signaling is insufficient to phenocopy GATA2 loss.

GATA2 Directly Regulates Rho Target Genes to Maintain Pathway Activity

To better understand how GATA2 maintains mutant NSCLC viability, we carried out ChIP-seq for GATA2 in mutant (A549 and PC9) and WT (H322M and H520) lung cancer cells. As corroboration of our ChIP-seq results, we assayed a set of peaks from the sequencing results across the four cell lines by ChIP-PCR and found occupancy with GATA2 (Figure S4A). Moreover, ChIP-PCR with a second, independent GATA2 antibody comparably enriched for several target genes from the ChIP-seq (Figure S4B), demonstrating the specificity of these targets for GATA2. Taken together, these findings validate the results of our ChIP-seq in a panel of lung cancer cell lines.

We then determined whether there was enrichment of gene sets particularly in mutant cells. Strikingly, we observed numerous Rho-related signaling pathways as being broadly occupied by GATA2 in mutant cells but not in WT cells (Figure S4C). Among these Rho-pathway genes is the Rho kinase ROCK1, as seen in Figure 5A. By ChIP-PCR, we verified that several of the Rho-pathway genes were bound by GATA2 in mutant but not WT NSCLC cells (Figure 5B). Furthermore, our original GSEA included Rho-related cell adhesion pathways among the GATA2-regulated gene sets (Figure S4D), and qRT-PCR revealed reduced expression of Rho-pathway targets with GATA2 depletion (Figure 5C). In total, these results suggest that GATA2 directly regulates expression of Rho-signaling components.

Recognizing this regulation of Rho targets by GATA2, we assessed the functional consequences of GATA2 loss on Rho activity. GATA2 knockdown triggered a striking decline in GTP-bound Rho (including RhoA, RhoB, and RhoC isoforms) in mutant lung cancer cells (Figure 5D). This was intriguing, as one of the GATA2-regulated Rho target genes was *EPHA3*, an ephrin receptor and upstream activator of Rho signaling (Pitulescu and Adams, 2010). Notably, depletion of *EPHA3* caused a reduction in GTP-bound Rho that was similar to the loss of GATA2, both at the steady state and in response to stimulation with Ephrin A5 (Figures S4E and S4F).

This effect on Rho-pathway activation was specific to RAS-pathway mutant lung cancer cells, as phosphorylation of the myosin light chain (pMLC), a substrate of ROCK1 and downstream marker for Rho signaling, was suppressed in mutant cells with GATA2 knockdown but was unaffected in WT cells (Figure 5E). To address the possibility that the effect on Rho signaling was due to apoptosis caused by GATA2 loss, we examined pMLC in GATA2-depleted cells in the presence of z-VAD. Importantly, pMLC was comparably suppressed in the presence of z-VAD (Figure S4G). Taken together, these effects demonstrate that GATA2 is necessary for Rho-pathway activation in RAS-pathway mutant NSCLC.

We explored the functional role for Rho in GATA2-mediated viability by pathway rescue. Constitutively active $RhoA^{G14V}$ fully restored Rho-GTP levels and pathway activity (Figure 5F). When we examined viability, activated Rho substantially rescued mutant cell survival in response to GATA2 depletion (Figure 5G). Interestingly, this rescue was reversed by the ROCK inhibitor fasudil, which efficiently abrogated pMLC (Figures S5A and S5B). In line with this, restoration of ROCK function via the ROCK:ER fusion also substantially restored viability in response to GATA2 depletion (Croft et al., 2004) (Figures S5C and S5D). We then examined whether the Rho pathway was individually necessary for RAS-pathway mutant cell survival. Depletion of ROCK1 had only marginal effects on mutant cell viability, in spite of robust suppression of pMLC (Figures S5E and S5F). Moreover, knockdown of a panel of Rho-pathway components or

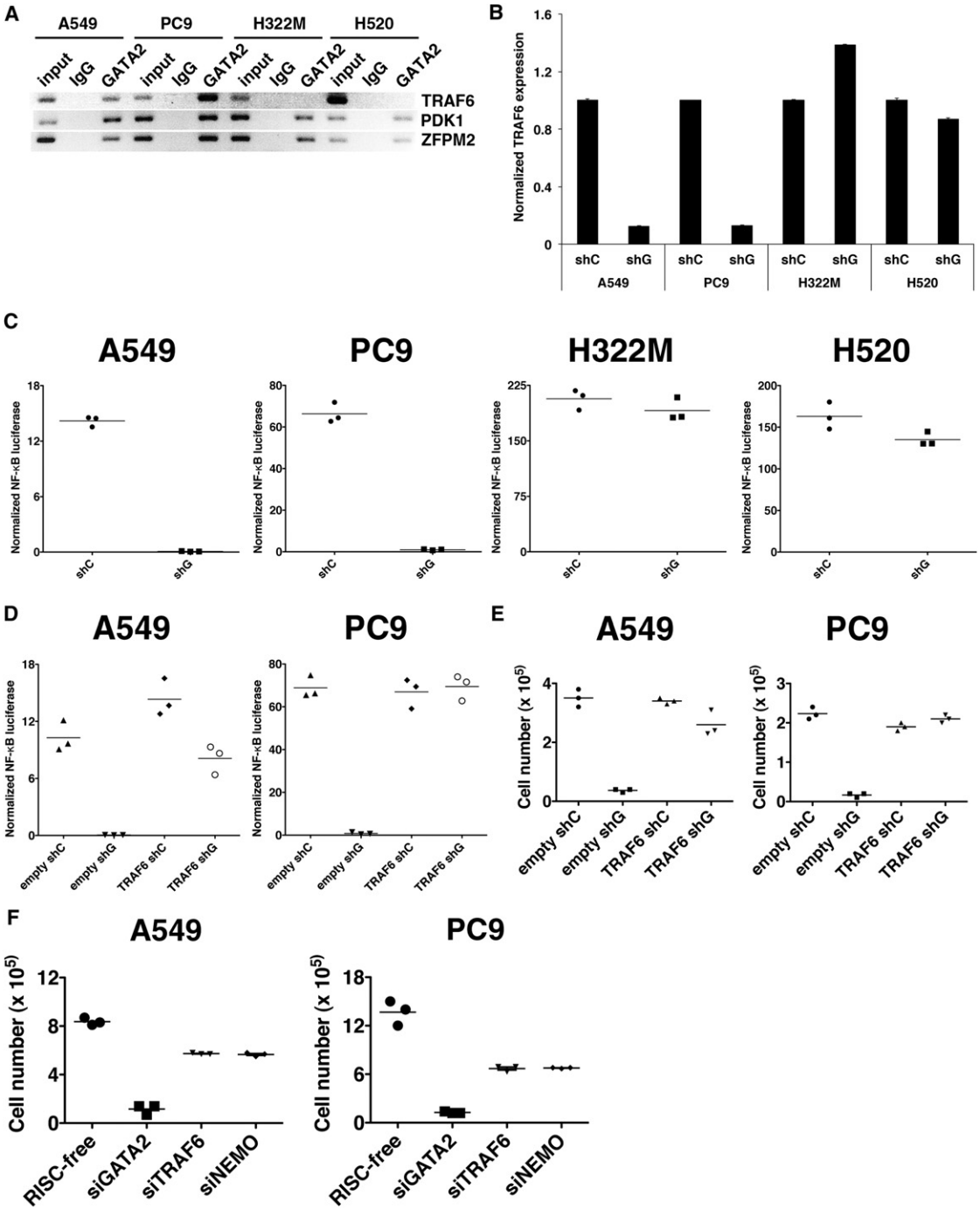

Figure 4. GATA2 Controls IL-1/NF-κB Signaling via TRAF6

(A) ChIP was performed with a control antibody (IgG) or an antibody for GATA2 in A549, PC9, H322M, and H520 cells, and PCR was performed for TRAF6, PDK1, and ZFPM2.

(B) qRT-PCR was performed for TRAF6 in A549, PC9, H322M, and H520 cells as in Figure 3A. Values are mean ± SEM (n = 3).

(C) NF-κB and control reporter plasmids were cotransfected into shRNA-infected A549, PC9, H322M, and H520 cells. Twenty-four hours later, luciferase assays were performed. Pathway activity was determined by normalizing luciferase from the NF-κB reporter to the control.

(D) NF-κB and control reporter plasmids were cotransfected into shRNA-infected A549 and PC9 cells expressing empty vector or TRAF6. Luciferase assays were performed as above.

(E) ShRNA-infected A549 and PC9 cells expressing empty vector or TRAF6 were plated and counted as in Figure 1D.

(F) A549 and PC9 cells were transfected with control siRNA or siRNAs targeting GATA2, TRAF6, or NEMO as in Figure 1B. Cell numbers were counted 72 hr later.

See also Figures S3, S4, and S6.

treatment with the ROCK inhibitor fasudil exhibited no differential viability in our panel of 26 NSCLC cell lines (Figures S5G and S5H). In sum, these results suggest that although Rho pathway activation is sufficient to rescue viability in response to GATA2 loss, it is not solely necessary for mutant NSCLC survival.

GATA2 Regulates Rho Target Genes via a STAT5 Transcriptional Complex

To understand how GATA2 differentially occupied Rho targets, we examined the DNA sequence motifs enriched in the mutant versus WT GATA2 ChIPs. Strikingly, we observed the STAT5 response element as specifically enriched in mutant cells (Hennighausen and Robinson, 2008) (Figure 5H). Thus, we predicted that GATA2 and STAT5 interact at Rho-pathway target genes. We first examined this putative GATA2/STAT5 interaction by coimmunoprecipitations of the factors and found that the factors did immunoprecipitate with one another in mutant but not WT cells (Figure 5I). Furthermore, as seen in Figure 5J, by ChIP/re-ChIP analyses, we found that GATA2 and STAT5 interact at Rho target gene loci particularly in mutant lung cancer cells. Importantly, whereas Rho target genes did not ChIP in a GATA2/STAT5 complex in WT cells, GATA2 targets common to mutant and WT lung cancer cells were enriched in all cells, demonstrating the capacity to isolate GATA2 targets in WT cells. Collectively, these results demonstrate that GATA2 is bound to Rho target genes via a complex with STAT5.

Considering the dependency on GATA2-regulated pathways in RAS-pathway mutant cancer cells, it was unclear whether GATA2 was regulated by activated oncogenes. To address this, we inhibited oncogenic EGFR in PC9 cells with the tyrosine kinase inhibitor erlotinib. Interestingly, although erlotinib treatment efficiently suppressed MAP kinase signaling, it did not affect STAT5 phosphorylation (Figure S5I). Consequently, erlotinib treatment had no effect on GATA2 occupancy of either IL-1 or Rho target genes (Figure S5J). To further explore the interaction of GATA2- and RAS-pathway signaling, we examined the effect of depleting KRAS on the GATA2 network. Notably, whereas KRAS knockdown did suppress phosphorylation of ERK and Akt, it did not affect proteasome activity, Rho signaling, or NF-κB activity (Figures S5K and S5L). Taken together, these results suggest that GATA2 operates orthogonally to RAS-pathway signaling.

To elucidate the differential occupancy of GATA2 in RAS-pathway mutant cells, we examined a panel of *KRAS* mutant, *EGFR* mutant, and WT NSCLC cell lines. This analysis revealed a trend toward higher levels of STAT5 phosphorylation in mutant versus WT cells (Figure S5M). Interestingly, expression of constitutively active STAT5 in WT cells was sufficient to drive GATA2 occupancy at Rho target genes (Figure S5N). We then examined whether STAT5 was individually required in RAS-pathway mutant NSCLC. Notably, we found that depletion of a single STAT5 isoform, STAT5B, was sufficient to both deplete total STAT5 and substantially suppress Rho signaling (Figure S5O). In addition, STAT5B knockdown caused a reduction in Rho target gene expression that was similar to the loss of GATA2 (Figure S5P). Yet knockdown of STAT5B caused only a modest decline in viability (Figure S5Q). In total, these findings indicate that STAT5, although necessary for Rho-pathway function, does not engender the same dependency as GATA2 itself in RAS-pathway mutant NSCLC.

The GATA2 Transcriptional Network Is General and Displays Considerable Crosstalk

Though the above results describe a dependency on GATA2-regulated pathways in two mutant lung cancers, we wanted to assess the extent of the GATA2 network in RAS-pathway mutant NSCLC. To do so, we examined GATA2-regulated pathways in three additional *KRAS* mutant and three additional WT lung cancer cells after GATA2 loss. Similar to the effects seen earlier, GATA2 depletion abrogated proteasome function across both genotypes (Figure S6A). Moreover, GATA2 loss inhibited Rho signaling and suppressed NF-κB activity only in *KRAS* mutant cells, as seen above (Figures S6A and S6B). In sum, these results show that GATA2-regulated pathways are broadly maintained in RAS-pathway mutant NSCLC.

Because of the striking dependency of mutant NSCLC on the GATA2 network, we examined whether there were interactions across GATA2-regulated pathways. Notably, we found control of NF-κB signaling by both the proteasome and Rho signaling, as activation of either was capable of restoring NF-κB activity with GATA2 loss (Figures S6C and S6D). These findings corroborate studies demonstrating an interaction of the proteasome and Rho pathways with NF-κB (Perona et al., 1997; Xue et al., 2011). Moreover, Rho signaling in response to GATA2 knockdown was rescued by activation of the IL-1 pathway with TRAF6 (Figure S6E). This is in line with earlier observations of various cytokines, including IL-1, stimulating Rho signaling (Sanz-Moreno et al., 2011). This Rho signal induction is the likely cause of the substantial rescue observed with TRAF6 expression after GATA2 depletion that is not recapitulated with activation of NF-κB alone. In contrast, activation of IL-1 or Rho signaling had no effect on proteasome function after GATA2 loss (Figure S6F). Collectively, these results outline a multifactorial GATA2 network in RAS-pathway mutant NSCLC (Figure 5K).

Gata2 Is Required for Oncogenic Kras-Driven Lung Tumorigenesis

To determine the relevance of this network in vivo, we conditionally deleted *Gata2* in an autochthonous model of *Kras* mutant NSCLC (Charles et al., 2006; Jackson et al., 2001). To do so, we generated $Kras^{LSL\text{-}G12D}$; $Gata2^{+/+,Flox/+,Flox/Flox}$ mice (hereafter referred to as KG +/+, F/+, and F/F mice, respectively) and infected their lungs with adenovirus that expresses Cre recombinase (Ad-Cre). Eight weeks after infection, we compared the cohort histopathologically and observed a very large reduction in tumor burden in KG F/F animals compared to both KG +/+ and F/+ controls (Figures 6A and 6B). Moreover, both KG F/+ and KG F/F mice exhibited a significant decrease in tumor number relative to KG +/+ controls, with KG F/F animals exhibiting a more striking decline (Figure 6C). In contrast, the average sizes of the tumors that did arise were comparable among KG +/+, F/+, and F/F mice (Figure 6D). To characterize the tumors in KG F/F mice, we prepared DNA from these lesions and analyzed recombination. Intriguingly, tumors from KG F/F mice retained an unrecombined floxed *Gata2* allele, whereas the *Kras* allele was completely recombined in the same lesions (Figure 6E).

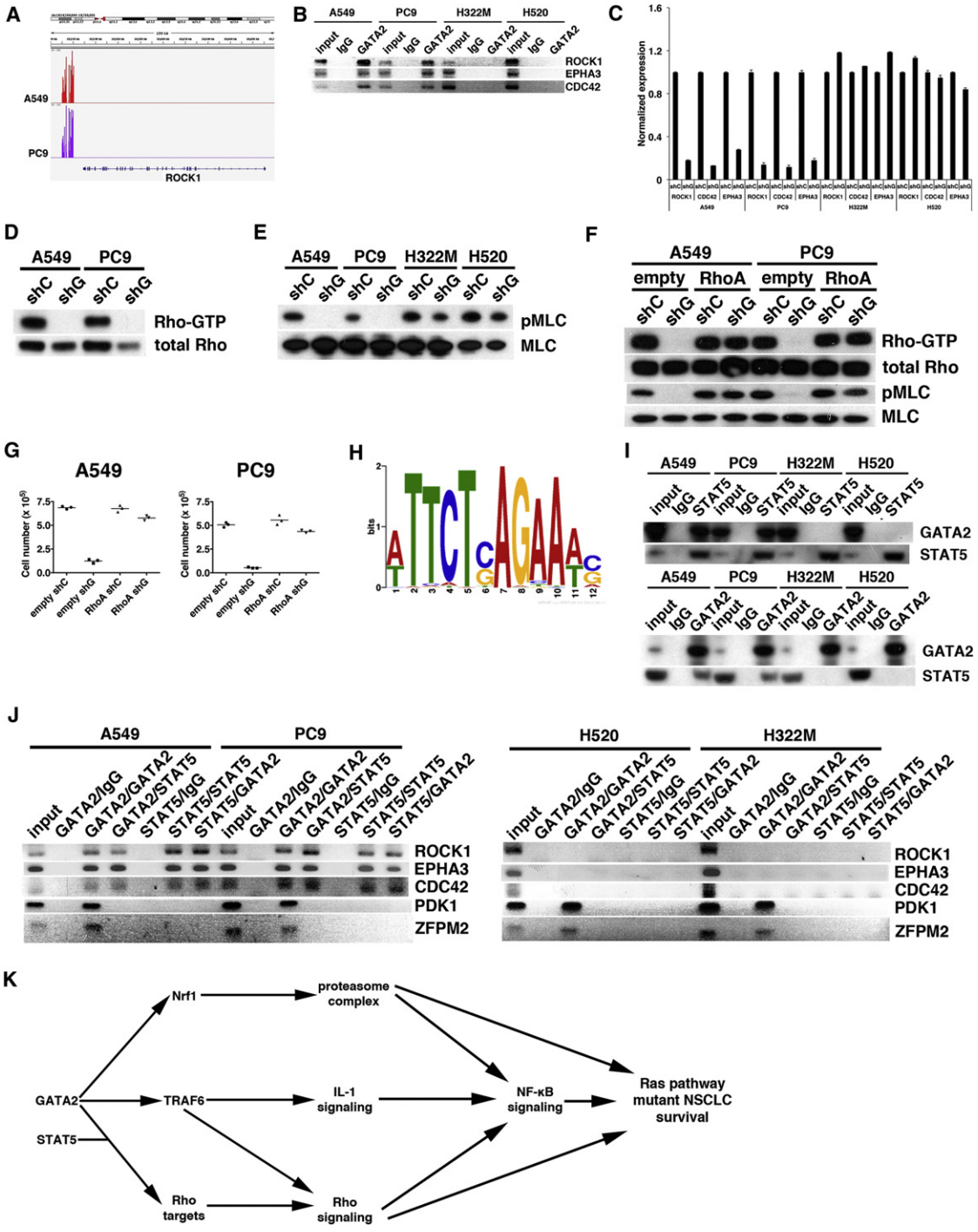

Figure 5. GATA2 Regulates Rho Pathway Signaling via a Transcriptional Complex with STAT5

(A) Representative GATA2 ChIP-seq images from the IGV Genome Browser for ROCK1 in A549 and PC9 cells.

(B) ChIP was performed in A549, PC9, H322M, and H520 cells as in Figure 4A, and PCR was performed for ROCK1, EPHA3, and CDC42.

(C) qRT-PCR was performed for ROCK1, EPHA3, and CDC42 as in Figure 3A. Values are mean ± SEM (n = 3).

(D) Rho-GTP pull-down assays were performed in shRNA-infected A549 and PC9 cells. Western blotting was performed on pull-downs (Rho-GTP) and total cell lysates (total Rho).

(E) Western blotting was performed on shRNA-infected A549, PC9, H322M, and H520 cells for pMLC and total MLC.

(F) Rho-GTP pull-down assays were performed in shRNA-infected A549 and PC9 cells expressing empty vector or $RhoA^{G14V}$ (RhoA). Western blotting was performed on pull-downs (Rho-GTP) and total cell lysates (total Rho, pMLC, and MLC).

(G) shRNA-infected A549 and PC9 cells expressing empty vector or $RhoA^{G14V}$ (RhoA) were plated and counted as in Figure 1D.

Taken together, these results indicate that *Gata2* is requisite for oncogenic *Kras*-driven lung tumor initiation.

Loss of Gata2-Induced Regression in Established *Kras* Mutant Tumors

Although the above findings suggest a role for *Gata2* in *Kras* mutant NSCLC, they do not demonstrate that *Gata2* is necessary for the maintenance of established *Kras* mutant lung tumors, only for their development. We thus generated $Kras^{LA2\text{-}G12D/+}$; $Rosa26^{CreERT2/+}$; $Gata2^{+/+,Flox/+,Flox/Flox}$ (hereafter referred to as LG +/+, F/+, and F/F mice, respectively). In these animals, lung tumors develop spontaneously from expression of mutant *Kras* due to spontaneous recombination (Johnson et al., 2001). We then induce whole-body deletion of *Gata2* using the CreERT2 conditional allele expressed from the *Rosa26* locus (Hameyer et al., 2007). After 3 days of tamoxifen treatment, we observed recombination of the *Gata2* locus in both organs and lung tumors of LG F/+ and F/F mice, along with *Kras* recombination in the lung tumors (Figure 6F). Western blot analysis revealed complete loss of GATA2 protein after 3 days of tamoxifen treatment in LG F/F lung tumors (Figure 6G). We also observed inhibition of the proteasome and Rho-signaling pathways in LG F/F lesions, along with elevation of the apoptotic marker cleaved caspase 3. In total, these findings show that tamoxifen treatment leads to efficient, whole-body *Gata2* locus recombination, with subsequent loss of GATA2 protein and inhibition of regulated pathways in lung tumors.

We then assessed the effect of *Gata2* loss on established lung lesions. We scanned animals by micro-CT the day before tamoxifen treatment and then treated animals for 1 week with tamoxifen. We then monitored animals by micro-CT for 1 month. As seen in Figures 6H and 6I, we found that *Gata2* loss had a striking effect, with near-complete abrogation of lung tumors in treated LG F/F mice. Longitudinal analysis of LG +/+ animals revealed a substantial increase in tumor size over time; a more modest increase in LG F/+ mice; and extensive regression in LG F/F mice (Figure 6J). Importantly, systemic *Gata2* loss was well tolerated as tamoxifen treatment of $Rosa26^{CreERT2/+}$; $Gata2^{+/+,F/+,F/F}$ mice revealed only a transient drop in body weight independent of *Gata2* genotype (Figure S7A). Although these results could be due partially to lost GATA2 function in the endothelial lineage (Kanki et al., 2011; Linnemann et al., 2011), these findings in *Kras* mutant NSCLC models demonstrate that *Gata2* not only affects tumor initiation but also triggers major regression in established lesions.

Combined Inhibition of the Proteasome and Rho Signaling Robustly Suppresses *Kras* Mutant Tumor Growth

Though cellular and genetic studies reveal a dependency on GATA2 for RAS-pathway mutant NSCLC, the known difficulty of targeting transcription factors with small molecules raises issues as to how to translate this into the clinical setting. However, our studies revealed a GATA2-regulated signaling network, several components of which can be inhibited with clinically available compounds. In particular, the proteasome, and indirectly NF-κB, can be inhibited with the FDA-licensed drug bortezomib and the Rho/ROCK-signaling cascade with fasudil, which has been approved for clinical use in Japan. To examine combined inhibition of these pathways on *KRAS* mutant NSCLC, we first treated a subset of *KRAS* mutant and WT cells with the individual drugs and their combination. Notably, whereas there was a substantial effect of combined bortezomib/fasudil treatment in mutant cells, the effect was much less pronounced in WT cells (Figure S7B). To exclude any potential off-target effects of these drugs, we also combined siRNAs targeting ROCK1 and various proteasome components in RAS-pathway mutant cells. Relative to control siRNAs or single pathway inhibition, mutual knockdown of ROCK1 and the proteasome combined to reduce mutant cell viability (Figure S7C). Collectively, these results provide a rationale for combining proteasome and Rho-pathway inhibition in *Kras* mutant NSCLC.

To extend these results in vivo, we treated $Kras^{LA2\text{-}G12D}$ mice at 12 weeks old, an age at which these animals have an extensive lung tumor burden (Johnson et al., 2001), with either drug individually or both in combination. We found that bortezomib and fasudil treatments for 3 days clearly suppress proteasome and ROCK signaling, respectively (Figure 7A). However, only combined treatment with bortezomib and fasudil elicited increased caspase 3 cleavage, demonstrating elevated apoptosis in those lesions. We then established a 4 week treatment protocol with bortezomib and fasudil individually or in combination. Notably, after 4 weeks of treatment, we still observed substantial repression of the proteasome and ROCK signaling in the lung (Figure S7D). Subsequent histopathological analysis of these animals revealed a modest decrease in tumorigenesis with bortezomib or fasudil treatment alone and a very substantial decrease in tumor growth with the combination (Figure 7B). Quantitation of these effects revealed major reductions in tumor burden, tumor number, and average tumor size with the combination therapy relative to both control and single-drug treatments (Figures 7C–7E). Although the effect of this combination on the stroma might also contribute to inhibition of tumor growth, as seen for ROCK/JAK inhibition in squamous cell cancers (Sanz-Moreno et al., 2011), our combined genetic and pharmacological analyses suggest a strong cell-autonomous effect of GATA2 pathway suppression on the tumor tissue, as in the $Kras^{LSL\text{-}G12D}$ model *Gata2* is deleted only in tumor cells and not stroma, endothelial, or other host tissues. Collectively, these results demonstrate that joint treatment with clinically available inhibitors causes substantial regression of *Kras*-mutant NSCLC.

(H) Meme analysis of A549 and PC9 GATA2 ChIP peaks reveals enrichment of the STAT5 response element.
(I) IPs were performed in A549, PC9, H322M, and H520 cells, and western blotting for GATA2 and STAT5 was performed on 5% total cell lysate (input) and the IPs.
(J) ChIP/re-ChIP was performed in A549, PC9, H520, and H322M cells, and PCR was performed for ROCK1, EPHA3, CDC42, PDK1, and ZFPM2.
(K) Model of GATA2 function in oncogene-driven NSCLC. GATA2 regulates a transcriptional network composed of the proteasome, IL-1-signaling, and Rho-signaling pathways, which maintain RAS-pathway mutant survival through NF-κB-dependent and NF-κB-independent mechanisms.
See also Figures S4, S5, and S6.

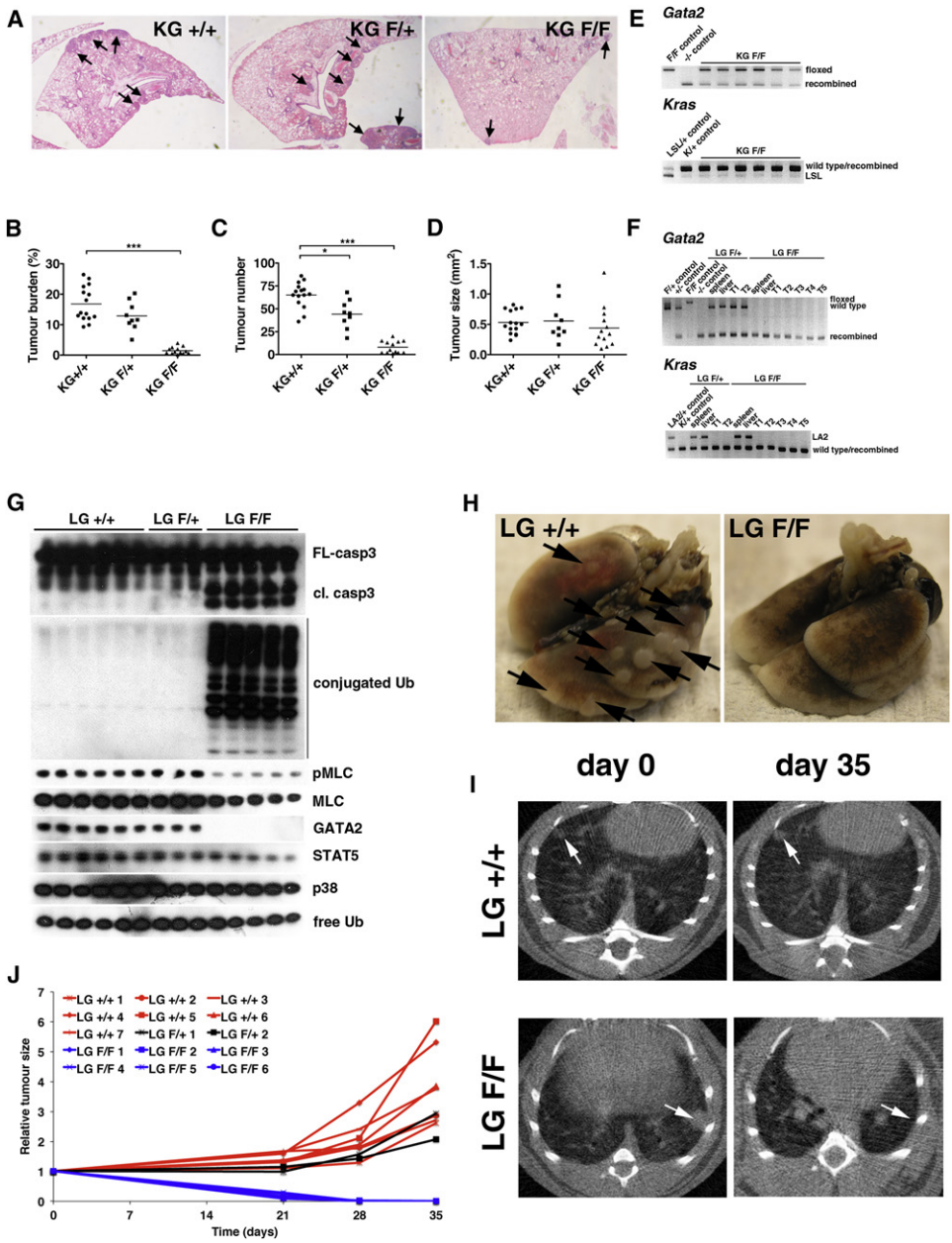

Figure 6. *Gata2* Is Required for *Kras*-Driven Autochthonous Lung Tumorigenesis

(A) Representative histological images of lungs from KG +/+, F/+, and F/F mice 8 weeks after infection with adenovirus that expresses Cre (Ad-Cre). Black arrows indicate lung adenomas. Magnification is 1×.

(B) Tumor burden (tumor area as a percentage of total lung area) in KG +/+ (n = 15), F/+ (n = 9), and F/F (n = 13) mice 8 weeks after Ad-Cre. ***$p < 0.0005$.

(C) Tumor number in the above mice 8 weeks after Ad-Cre. *$p < 0.05$; ***$p < 0.0005$.

(D) Tumor size in the above mice 8 weeks after Ad-Cre.

(E) *Gata2* and *Kras* recombination was assessed in KG F/F lung tumors. $Gata2^{F/F}$ (F/F control) and $Gata2^{-/-}$ (−/− control) tissues served as controls for *Gata2*. $Kras^{LSL\text{-}G12D}$ (LSL/+ control) and $Kras^{G12D}$ (K/+ control) mouse embryonic fibroblasts (MEFs) served as controls for *Kras*.

(F) *Gata2* and *Kras* recombination was assessed in LG F/+ and F/F animals. Mice were fed a tamoxifen diet for 3 days. Animals were culled, and spleen, liver, and lung tumor DNA was analyzed. $Gata2^{F/+}$ (F/+ control), $Gata2^{+/-}$ (+/− control), $Gata2^{F/F}$ (F/F control), and $Gata2^{-/-}$ (−/− control) tissues served as controls for *Gata2*. $Kras^{LA2\text{-}G12D}$ (LA2/+ control) tissue and LKR13 (K/+ control) cells served as controls for *Kras*.

(G) GATA2 loss and pathway modulation were assessed in LG +/+, F/+, and F/F animals. Mice were fed a tamoxifen diet for 3 days. Animals were culled, and lung tumor lysates analyzed. Western blotting was performed for caspase 3 (full-length [FL] and cleaved), ubiquitin (conjugated and free), STAT5, GATA2, p38, pMLC, and MLC.

(H) Representative LG +/+ and F/F lungs after tamoxifen diet. Animals were fed a tamoxifen diet for a week, monitored for 28 days, and then sacrificed. Black arrows indicate lung tumors.

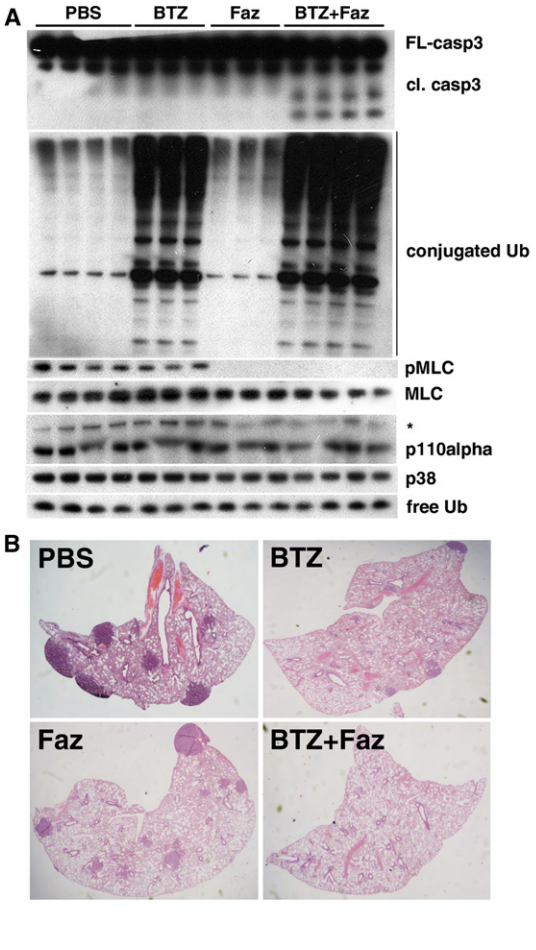

Figure 7. Combined Inhibition of the Proteasome and Rho Signaling Recapitulates the Effect of GATA2 Loss on Oncogenic *Kras*-Driven Tumorigenesis

(A) Twelve-week-old $Kras^{LA2\text{-}G12D}$ animals were treated with PBS, bortezomib (BTZ), fasudil (Faz), or bortezomib and fasudil (BTZ+Faz). After 3 days, animals were culled, and western blotting was performed on lung tumors for caspase 3 (full-length [FL] and cleaved), ubiquitin (conjugated and free), p110alpha, p38, pMLC, and MLC. * represents a nonspecific band detected with p110alpha.

(B) Representative histological images of lungs from $Kras^{LA2\text{-}G12D}$ mice treated with PBS, BTZ, Faz, or BTZ+Faz for 4 weeks, starting at 12 weeks of age. Magnification is 1×.

(C) Tumor burden in mice treated with PBS (n = 11), BTZ (n = 10), Faz (n = 10), or BTZ+Faz (n = 10) for 4 weeks, starting at 12 weeks of age. *p < 0.05; **p < 0.005; ***p < 0.0005.

(D) Tumor number in mice from (C). **p < 0.005; ***p < 0.0005.

(E) Tumor size in mice from (C). *p < 0.05; **p < 0.005; ***p < 0.0005.

See also Figure S7.

DISCUSSION

The GATA2 Transcriptional Network Regulates RAS-Pathway Mutant NSCLC Survival

In this report, we have shown that lung cancers with mutations in *KRAS* and other oncogenes on the RTK/RAS pathway depend upon GATA2 for survival. Through integrated analyses of gene expression and genome occupancy, we found that this dependency occurs via concurrent regulation of three pathways: the proteasome machinery; the IL-1/NF-κB signaling pathway; and the Rho-signaling cascade (Figure 5K). These pathways exhibit extensive crosstalk, suggesting the network to be mutually reinforcing (Figures S6C–S6E). Interestingly, the proteasome has been shown in several earlier screens to be a specific *KRAS* dependency (Barbie et al., 2009; Luo et al., 2009). Our results are in line with this, though we found that neither loss of individual proteasome components nor proteasome inhibition differentially reduces *KRAS* mutant cell viability (Figures S2D and S2E). Furthermore, the NF-κB pathway has been previously described as required in KRAS-driven lung cancer in vitro and in vivo (Barbie et al., 2009; Meylan et al., 2009). We have seen a similar coordination of NF-κB- and RAS-pathway mutant cell survival, though we find that NF-κB inhibition is neither necessary nor sufficient for mutant NSCLC-specific killing (Figures 4F and S3F–SJ).

An intriguing discovery was the control of Rho signaling by GATA2 in complex with STAT5. Earlier work from Marshall and colleagues described interdependence between RAS and Rho signaling in oncogenic transformation (Olson et al., 1998). Moreover, an earlier *KRAS* synthetic lethal screen found the ephrin receptor EPHA6 to be specifically required in *KRAS* mutant lung cancer cells (Barbie et al., 2009), and recent resequencing has described mutations of multiple ephrin receptors in lung adenocarcinoma (Ding et al., 2008). As the Rho pathway is a major effector of ephrin signaling (Pitulescu and Adams, 2010), these changes provide a basis for Rho dependency in NSCLC.

Our findings expand the role of GATA2-regulated pathways to include RAS-pathway oncogene-mutated lung cancers.

(I) Representative transaxial images of LG +/+ and F/F lungs before and after tamoxifen diet. Animals were initially scanned by micro-CT (day 0) and fed a tamoxifen diet for a week. After 2 weeks, animals were scanned once weekly for 3 weeks until sacrifice (day 35). White arrows indicate detectable lesions at days 0 and 35.

(J) Longitudinal quantification of LG lung tumors over time as described above. Tumor volumes from day 0 are set to 1, and relative tumor sizes were recorded. Red, black, and blue lines correspond to LG +/+ (n = 3 animals), F/+ (n = 2 animals), and F/F (n = 3 animals) tumors, respectively.

See also Figure S7.

Intuitively, general dependencies in the RAS/RTK pathway should occur, as these factors share a common signaling axis. Moreover, resequencing of various cancers with mutations in the RAS/RTK cascade have found mutations in these components to be mutually exclusive, suggesting that they engender a common effect (Ding et al., 2008). Surprisingly, we found that GATA2 operates orthogonally to oncogenes, as suppression of oncogenic signaling did not affect GATA2 genome occupancy or regulated pathway function (Figures S5I–S5L). GATA2 has no known oncogenic function in its own right and is not controlled by signals emanating from the RTK/RAS pathway. Thus, dependency on the GATA2 transcriptional network might evolve as a stress-response mechanism in parallel to oncogene signaling during tumorigenesis, and that selection for the network in RAS-pathway mutant cells eventually converts into dependency on continued GATA2 function, a form of nononcogene addiction.

Elucidation of the GATA2 Transcriptional Network Exposes a Multiplicity of Druggable Intervention Points

Our investigations revealed a marked attenuation of autochthonous *Kras* mutant NSCLC growth in response to systemic *Gata2* loss; similar effects were observed with whole-body inhibition of the Myc-Max interaction in a related *Kras* mutant lung tumor model (Soucek et al., 2008). However, these findings face the issue of translation into clinically relevant therapies, as DNA-binding proteins are traditionally considered undruggable by the pharmaceutical industry (Darnell, 2002).

Through integrated analyses of gene expression and genome occupancy, we defined a GATA2 network of signaling pathways that present discrete avenues of therapeutic targeting. Consequently, we combined inhibition of the proteasome and Rho/ROCK signaling with the clinical compounds bortezomib and fasudil, respectively. Considering the dramatic effects observed with this regimen, we believe such a strategy may benefit patients with RAS-pathway mutant NSCLC.

Beyond this initial approach, such treatment strategies could be improved further by inhibition of IL-1 signaling with IL-1 receptor monoclonal antibodies (Dinarello, 2010). Moreover, as this approach targets a network, one could envisage a multitiered strategy to inhibit various points within the signaling pathways. For example, along with fasudil one could inhibit Rho signaling upstream at the ephrin receptor with dasatinib (Montero et al., 2011). Finally, as GATA2 functions with STAT5 (Hennighausen and Robinson, 2008), a transcription factor regulated by phosphorylation, it would be intriguing to determine its regulatory kinase or kinases, as these factors might serve as therapeutic targets. We anticipate that this report will extend the basis for combinatorial design of targeted therapies in lung cancer.

EXPERIMENTAL PROCEDURES

Detailed procedures are described in the Extended Experimental Procedures.

ChIP-Seq

ChIP assays were performed as described (Valouev et al., 2008). Both ChIP samples and total chromatin were submitted for Illumina sequencing as described (Schmidt et al., 2009). Details of computational analyses are in the Extended Experimental Procedures.

Mouse Strains

$Kras^{LSL\text{-}G12D}$ and $Kras^{LA2\text{-}G12D}$ mice were from the Mouse Models of Human Cancer Consortium (Johnson et al., 2001; Tuveson et al., 2004). $Rosa26^{CreERT2}$ mice were from A. Berns (Hameyer et al., 2007). $Gata2^{F}$ mice were from the Mutant Mouse Regional Resource Center (Charles et al., 2006). BALB/C nude mice were from Charles River Laboratories. Animal husbandry details are in the Extended Experimental Procedures.

Tamoxifen Treatment

Mice were given a tamoxifen diet as described (Blasco et al., 2011). Further details are in the Extended Experimental Procedures.

Micro-CT Analysis

Micro-CT analysis was performed with the SkyScan 1176. LG mice were scanned, given a tamoxifen diet for 1 week, and scanned weekly. Details are in the Extended Experimental Procedures.

Drug Treatment In Vivo

Mice were treated with PBS, bortezomib, fasudil, or bortezomib and fasudil. For 3 day treatments, tumor protein was collected. For 4 week treatments, lungs were examined histologically or lung protein was collected. Details are in the Extended Experimental Procedures.

Statistical Analysis

Values represent mean ± standard error of the mean (SEM). For the NSCLC cell panel, significance was assessed with the Mann-Whitney test. For correlation analyses, significance was assessed with the Pearson's coefficient. For the cell cycle, significance was analyzed via chi-square testing. For qRT-PCR, error was propagated using standard methods. For histopathology, significance was determined using the Student's t test. For GSEA, significance was determined using an empirical phenotype-based permutation test as described (Subramanian et al., 2005). For GeneGo pathway enrichment, statistical significance was assessed with t statistics.

SUPPLEMENTAL INFORMATION

Supplemental Information includes Extended Discussion, Extended Experimental Procedures, seven figures, and one table and can be found with this article online at doi:10.1016/j.cell.2012.02.059.

ACKNOWLEDGMENTS

We thank S.M. Henshall for the GATA2 expression vector; D. Finley for the USP14 expression vector; R. Deshaies for the Nrf1 expression vector; D. Goubau for the NF-κB and control reporter plasmids; E. Meylan and W. Xue for the RelA expression vector; E. Sahai for the RhoA and ROCK:ER expression vectors; and F. Gouilleux for the $STAT5^{CA}$ expression vector. We thank the LRI FACS facility for cell-cycle assays and the Bart's Genome Centre for gene expression analysis. We thank C. Sheridan for micro-CT assistance. M.S.K. is a Long-Term Fellow of the Human Frontier Science Program and European Molecular Biology Organization. M.M. is a Marie Curie Postdoctoral Fellow. This work was supported by Cancer Research UK and by funding from the European Commission's Seventh Framework Programme (FP7/2007-2013) under the Lungtarget Grant agreement (HEALTH-F2-2010-259770).

Received: October 3, 2011
Revised: January 4, 2012
Accepted: February 29, 2012
Published: April 26, 2012

REFERENCES

Barbie, D.A., Tamayo, P., Boehm, J.S., Kim, S.Y., Moody, S.E., Dunn, I.F., Schinzel, A.C., Sandy, P., Meylan, E., Scholl, C., et al. (2009). Systematic RNA interference reveals that oncogenic KRAS-driven cancers require TBK1. Nature *462*, 108–112.

Blasco, R.B., Francoz, S., Santamaría, D., Cañamero, M., Dubus, P., Charron, J., Baccarini, M., and Barbacid, M. (2011). c-Raf, but not B-Raf, is essential for development of K-Ras oncogene-driven non-small cell lung carcinoma. Cancer Cell *19*, 652–663.

Cao, Z., Xiong, J., Takeuchi, M., Kurama, T., and Goeddel, D.V. (1996). TRAF6 is a signal transducer for interleukin-1. Nature *383*, 443–446.

Charles, M.A., Saunders, T.L., Wood, W.M., Owens, K., Parlow, A.F., Camper, S.A., Ridgway, E.C., and Gordon, D.F. (2006). Pituitary-specific Gata2 knockout: effects on gonadotrope and thyrotrope function. Mol. Endocrinol. *20*, 1366–1377.

Chien, Y., Kim, S., Bumeister, R., Loo, Y.M., Kwon, S.W., Johnson, C.L., Balakireva, M.G., Romeo, Y., Kopelovich, L., Gale, M., Jr., et al. (2006). RalB GTPase-mediated activation of the IkappaB family kinase TBK1 couples innate immune signaling to tumor cell survival. Cell *127*, 157–170.

Croft, D.R., Sahai, E., Mavria, G., Li, S., Tsai, J., Lee, W.M., Marshall, C.J., and Olson, M.F. (2004). Conditional ROCK activation in vivo induces tumor cell dissemination and angiogenesis. Cancer Res. *64*, 8994–9001.

Darnell, J.E., Jr. (2002). Transcription factors as targets for cancer therapy. Nat. Rev. Cancer *2*, 740–749.

Dinarello, C.A. (2010). Why not treat human cancer with interleukin-1 blockade? Cancer Metastasis Rev. *29*, 317–329.

Ding, L., Getz, G., Wheeler, D.A., Mardis, E.R., McLellan, M.D., Cibulskis, K., Sougnez, C., Greulich, H., Muzny, D.M., Morgan, M.B., et al. (2008). Somatic mutations affect key pathways in lung adenocarcinoma. Nature *455*, 1069–1075.

Engelman, J.A., Chen, L., Tan, X., Crosby, K., Guimaraes, A.R., Upadhyay, R., Maira, M., McNamara, K., Perera, S.A., Song, Y., et al. (2008). Effective use of PI3K and MEK inhibitors to treat mutant Kras G12D and PIK3CA H1047R murine lung cancers. Nat. Med. *14*, 1351–1356.

Ferlay, J., Shin, H.R., Bray, F., Forman, D., Mathers, C., and Parkin, D.M. (2010). Estimates of worldwide burden of cancer in 2008: GLOBOCAN 2008. Int. J. Cancer *127*, 2893–2917.

Hameyer, D., Loonstra, A., Eshkind, L., Schmitt, S., Antunes, C., Groen, A., Bindels, E., Jonkers, J., Krimpenfort, P., Meuwissen, R., et al. (2007). Toxicity of ligand-dependent Cre recombinases and generation of a conditional Cre deleter mouse allowing mosaic recombination in peripheral tissues. Physiol. Genomics *31*, 32–41.

Hennighausen, L., and Robinson, G.W. (2008). Interpretation of cytokine signaling through the transcription factors STAT5A and STAT5B. Genes Dev. *22*, 711–721.

Jackson, E.L., Willis, N., Mercer, K., Bronson, R.T., Crowley, D., Montoya, R., Jacks, T., and Tuveson, D.A. (2001). Analysis of lung tumor initiation and progression using conditional expression of oncogenic K-ras. Genes Dev. *15*, 3243–3248.

Johnson, L., Mercer, K., Greenbaum, D., Bronson, R.T., Crowley, D., Tuveson, D.A., and Jacks, T. (2001). Somatic activation of the K-ras oncogene causes early onset lung cancer in mice. Nature *410*, 1111–1116.

Kanki, Y., Kohro, T., Jiang, S., Tsutsumi, S., Mimura, I., Suehiro, J., Wada, Y., Ohta, Y., Ihara, S., Iwanari, H., et al. (2011). Epigenetically coordinated GATA2 binding is necessary for endothelium-specific endomucin expression. EMBO J. *30*, 2582–2595.

Lee, B.H., Lee, M.J., Park, S., Oh, D.C., Elsasser, S., Chen, P.C., Gartner, C., Dimova, N., Hanna, J., Gygi, S.P., et al. (2010). Enhancement of proteasome activity by a small-molecule inhibitor of USP14. Nature *467*, 179–184.

Linnemann, A.K., O'Geen, H., Keles, S., Farnham, P.J., and Bresnick, E.H. (2011). Genetic framework for GATA factor function in vascular biology. Proc. Natl. Acad. Sci. USA *108*, 13641–13646.

Luo, J., Emanuele, M.J., Li, D., Creighton, C.J., Schlabach, M.R., Westbrook, T.F., Wong, K.K., and Elledge, S.J. (2009). A genome-wide RNAi screen identifies multiple synthetic lethal interactions with the Ras oncogene. Cell *137*, 835–848.

Meylan, E., Dooley, A.L., Feldser, D.M., Shen, L., Turk, E., Ouyang, C., and Jacks, T. (2009). Requirement for NF-kappaB signalling in a mouse model of lung adenocarcinoma. Nature *462*, 104–107.

Montero, J.C., Seoane, S., Ocaña, A., and Pandiella, A. (2011). Inhibition of SRC family kinases and receptor tyrosine kinases by dasatinib: possible combinations in solid tumors. Clin. Cancer Res. *17*, 5546–5552.

O'Neill, L.A. (2008). The interleukin-1 receptor/Toll-like receptor superfamily: 10 years of progress. Immunol. Rev. *226*, 10–18.

Olson, M.F., Paterson, H.F., and Marshall, C.J. (1998). Signals from Ras and Rho GTPases interact to regulate expression of p21Waf1/Cip1. Nature *394*, 295–299.

Perona, R., Montaner, S., Saniger, L., Sánchez-Pérez, I., Bravo, R., and Lacal, J.C. (1997). Activation of the nuclear factor-kappaB by Rho, CDC42, and Rac-1 proteins. Genes Dev. *11*, 463–475.

Pitulescu, M.E., and Adams, R.H. (2010). Eph/ephrin molecules—a hub for signaling and endocytosis. Genes Dev. *24*, 2480–2492.

Puyol, M., Martín, A., Dubus, P., Mulero, F., Pizcueta, P., Khan, G., Guerra, C., Santamaría, D., and Barbacid, M. (2010). A synthetic lethal interaction between K-Ras oncogenes and Cdk4 unveils a therapeutic strategy for non-small cell lung carcinoma. Cancer Cell *18*, 63–73.

Radhakrishnan, S.K., Lee, C.S., Young, P., Beskow, A., Chan, J.Y., and Deshaies, R.J. (2010). Transcription factor Nrf1 mediates the proteasome recovery pathway after proteasome inhibition in mammalian cells. Mol. Cell *38*, 17–28.

Sanz-Moreno, V., Gaggioli, C., Yeo, M., Albrengues, J., Wallberg, F., Viros, A., Hooper, S., Mitter, R., Féral, C.C., Cook, M., et al. (2011). ROCK and JAK1 signaling cooperate to control actomyosin contractility in tumor cells and stroma. Cancer Cell *20*, 229–245.

Schmidt, D., Wilson, M.D., Spyrou, C., Brown, G.D., Hadfield, J., and Odom, D.T. (2009). ChIP-seq: using high-throughput sequencing to discover protein-DNA interactions. Methods *48*, 240–248.

Soucek, L., Whitfield, J., Martins, C.P., Finch, A.J., Murphy, D.J., Sodir, N.M., Karnezis, A.N., Swigart, L.B., Nasi, S., and Evan, G.I. (2008). Modelling Myc inhibition as a cancer therapy. Nature *455*, 679–683.

Subramanian, A., Tamayo, P., Mootha, V.K., Mukherjee, S., Ebert, B.L., Gillette, M.A., Paulovich, A., Pomeroy, S.L., Golub, T.R., Lander, E.S., and Mesirov, J.P. (2005). Gene set enrichment analysis: a knowledge-based approach for interpreting genome-wide expression profiles. Proc. Natl. Acad. Sci. USA *102*, 15545–15550.

Tuveson, D.A., Shaw, A.T., Willis, N.A., Silver, D.P., Jackson, E.L., Chang, S., Mercer, K.L., Grochow, R., Hock, H., Crowley, D., et al. (2004). Endogenous oncogenic K-ras(G12D) stimulates proliferation and widespread neoplastic and developmental defects. Cancer Cell *5*, 375–387.

Valouev, A., Johnson, D.S., Sundquist, A., Medina, C., Anton, E., Batzoglou, S., Myers, R.M., and Sidow, A. (2008). Genome-wide analysis of transcription factor binding sites based on ChIP-Seq data. Nat. Methods *5*, 829–834.

Vicent, S., Chen, R., Sayles, L.C., Lin, C., Walker, R.G., Gillespie, A.K., Subramanian, A., Hinkle, G., Yang, X., Saif, S., et al. (2010). Wilms tumor 1 (WT1) regulates KRAS-driven oncogenesis and senescence in mouse and human models. J. Clin. Invest. *120*, 3940–3952.

Xue, W., Meylan, E., Oliver, T.G., Feldser, D.M., Winslow, M.M., Bronson, R.T., and Jacks, T. (2011). Response and resistance to NF-κB inhibitors in mouse models of lung adenocarcinoma. Cancer Discov *1*, 236–247.

Yamaoka, S., Courtois, G., Bessia, C., Whiteside, S.T., Weil, R., Agou, F., Kirk, H.E., Kay, R.J., and Israël, A. (1998). Complementation cloning of NEMO, a component of the IkappaB kinase complex essential for NF-kappaB activation. Cell *93*, 1231–1240.